sustainability

MDPI

Article

Geochemical and Morphological Evaluations of Organic and Mineral Aerosols in Coal Mining Areas: A Case Study of Santa Catarina, Brazil

Segun A. Akinyemi [1,*], Marcos L. S. Oliveira [2,3], Bemgba B. Nyakuma [4] and Guilherme L. Dotto [5]

[1] Department of Geology, Faculty of Science, Ekiti State University, Ado Ekiti 362103, Nigeria
[2] Department of Civil and Environmental Engineering, Universidad de la Costa, Calle 58 #55-66, Barranquilla 080002, Atlántico, Colombia; marcos.oliviera@cuc.de
[3] Department of Sanitary and Environmental Engineering, Federal University of Santa Catarina, Florianópolis 88040-900, Brazil
[4] Department of Chemistry, Faculty of Sciences, Benue State University, Makurdi 970101, Nigeria; bbnyax1@gmail.com
[5] Department of Chemical Engineering, Federal University of Santa Maria, Santa Maria 97105-900, Brazil; guilherme_dotto@yahoo.com.br
* Correspondence: akinyemi70@gmail.com

Abstract: Numerous researchers have described the correlation between the short-term contact of nano-particulate (NP) matter in diverse coal phases and amplified death or hospitalizations for breathing disorders in humans. However, few reports have examined the short-term consequences of source-specific nanoparticles (NPs) on coal mining areas. Advanced microscopic techniques can detect the ultra-fine particles (UFPs) and nanoparticles that contain potential hazardous elements (PHEs) generated in coal mining areas. Secondary aerosols that cause multiple and complex groups of particulate matter (PM_{10}, $PM_{2.5}$, PM_1) can be collected on dry deposition. In this study, scanning electron microscopy (SEM) and high-resolution transmission electron microscopy (HR-TEM) were employed to detect and define the magnitude of particulate matters on restaurants walls at coal mines due to weathering interactions. The low cost self-made passive sampler (SMPS) documented several minerals and amorphous phases. The results showed that most of the detected coal minerals exist in combined form as numerous complexes comprising significant elements (e.g., Al, C, Fe, K, Mg, S, and Ti), whereas others exist as amorphous or organic compounds. Based on the analytical approach, the study findings present a comprehensive understanding of existing potential hazardous elements in the nanoparticles and ultrafine particles from coal mining areas in Brazil.

Keywords: geochemical; organic minerals; aerosols; coal mining; nanoparticles; ultrafine nanoparticles; Brazil

Citation: Akinyemi, S.A.; Oliveira, M.L.S.; Nyakuma, B.B.; Dotto, G.L. Geochemical and Morphological Evaluations of Organic and Mineral Aerosols in Coal Mining Areas: A Case Study of Santa Catarina, Brazil. *Sustainability* **2022**, *14*, 3847. https://doi.org/10.3390/su14073847

Academic Editors: Luis F.O. Silva and Hongya Niu

Received: 6 December 2021
Accepted: 21 March 2022
Published: 24 March 2022

1. Introduction

In coal mining areas, airborne contaminants are released during the operation of mines. Similarly, after the abandonment of the mines, such contaminants are further emitted from spontaneous coal combustions resulting in severe impacts on human health [1,2]. According to the latest World Health Organization (WHO), more than 8 million people die annually from anthropogenic air contamination, making it a significant environmental hazard. Air contamination is documented as a deadly pollutant that causes severe and prolonged disorders such as cardiovascular disease and chronic lung infections [3,4]. In searching scientific databases such as Scopus and Web of Science for the search strings; "coal impact" and "human health", over 10,000 publications were retrieved. However, there are no studies on particulate matter (PM) suspended at respiratory heights for humans. However, there have been some attempts to explore this area of research in Europe and the USA [5,6]. In addition, most studies in scientific bases for atmospheric studies require significantly

expensive equipment [7,8]. Furthermore, the traditional PM_{10}, $PM_{2.5}$ and PM_1 equipment are not as accurate as smaller particles are always detected in larger filters [9]. However, these above stated challenges motivate novel ideas for sample collection using self-made passive sampler (SMPS) in areas of coal mining, mainly where coal fires are prevalent. In times past, much anxieties have been concentrated on the prevention of unexpected accidents rather than on the harmful impact of coal dust on the human health [10,11]. Over the last few years, social and technological progress has led to increase health awareness and an escalating significance on dust reduction in coal mines. The documentation of the characteristics of coal mine dust is necessary to prevent dust explosion and occupational disease. The systematic study of the coal dust chemical nature and composition is related to personal health, production safety and environmental air quality [12]. In addition, it is an important step toward achieving dust control within the vicinity of coal mines.

Several studies have previously signaled that transitional elements such as bioavailable iron or nickel are culpable for the incidence of severe health problems [13–16]. However, the precise chemical nature and compositional information about the materials inhaled in coal mining areas remain scanty [17–19]. This knowledge gap is mainly because most published works on coal and potentially hazardous elements (PHEs) geochemistry focus on the toxic emissions and residues produced during combustion in coal power plants [19,20].

Therefore, in this paper, we focus on the PM inhaled by miners and identify the major PHEs that are present in coal mine dust. Furthermore, the paper presents an exploratory pilot case study that demonstrates how dust chemistry can change when PM size decreases. Lastly, this work presents further studies on the self-made passive sampler (SMPS) previously reported by Silva et al. [21]. In this paper, the SMPS was applied to collect multiple ultra-fine particles (UFPs) and nanoparticles (NPs) in direction to better comprehend the incidence of potential hazardous elements (PHEs) from a coal mining area in Brazil.

2. Materials and Methods

2.1. Sampling Strategy

The self-made passive sampler previously reported by Silva et al. [21] (see Figure 1) was mounted in the restaurants where miners typically take lunch. Sampling was conducted from 18 May 2019 to 23 August 2019 (winter months) by using the self-made passive sampler. After sampling, all the PMs were wrapped in plastic bags and deposited in a freezer (−18 °C) to avoid sunlight and studied for geochemical properties within one month. This approach facilitated realistic exposure to the PM collected and analyzed in this study.

For this study, the self-made passive sampler was placed at 1.50 m considering that the average height of miners (male and female) was 1.60 m. Therefore, the set-up was aimed at modelling the probable respiratory exposure of restaurant-goers in coal areas. In addition, the objective was to detect the incidence of the PHEs and directly reporting the findings by developing a low cost self-designed passive sampling procedure. The non-destructive plan adopted in the study was based on the procedure of advanced microscopy (AM) and X-ray diffraction (XRD) analyses. The designed self-made passive sampler comprises a PVC tube with an inner pin stub covered with carbon tape (Figure 1). Based on the wind and the environment of the cassettes, the UFPs and NPs are naturally deposited on the carbon tapes attached to the self-made passive sampler [21] accumulated PMs on the pin stub were subsequently examined without any pre-handling in the advanced microscopy (AM) workroom. Lastly, the influence of coal mining contamination and apparent dry sedimentations (due to high mining activities) on miners in restaurants was critically examined.

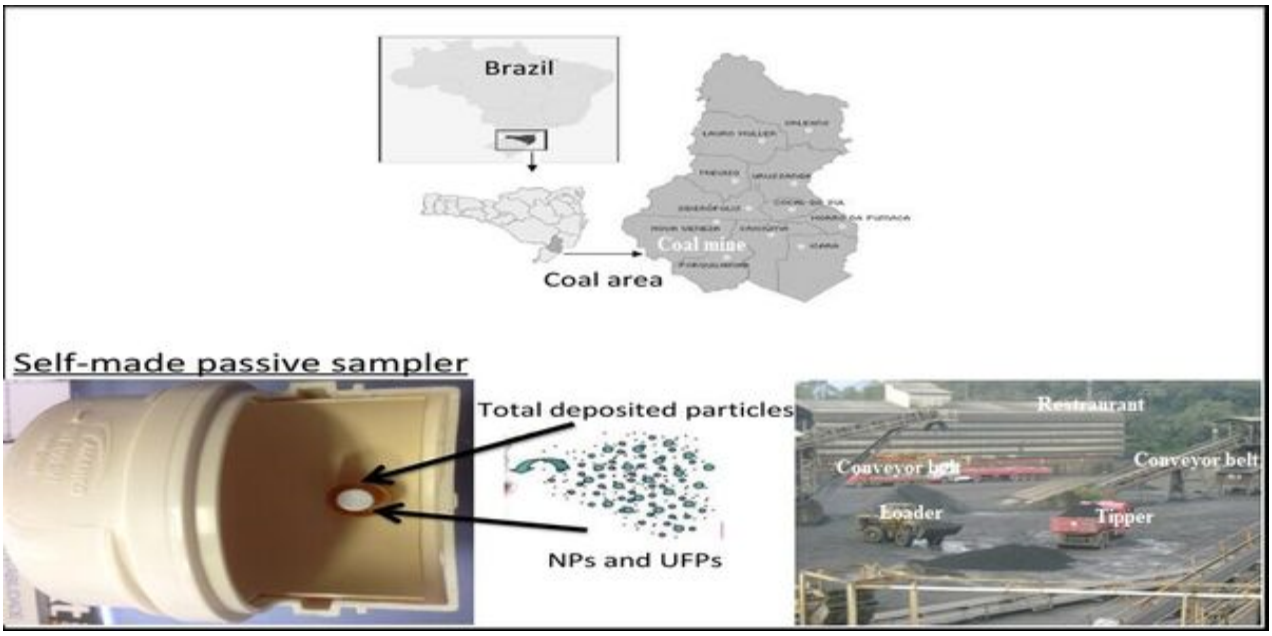

Figure 1. Studied zone and SMPS functions illustration.

2.2. Analytical Procedures

Current sampling equipment for detecting PM_{10}, $PM_{2.5}$, and PM_1 are considered inefficient [9,22]. Hence, the present study presents an attempt to detect and examine the total untreated particles or sample preparations that affect the chemical and mineralogical compositions of sampled PM. Consequently, field emission scanning electron microscopy (FE-SEM), and Focused Ion Beam (FIB) techniques were adopted to evaluate nano-compound assemblages. Likewise, high-resolution transmission electron microscopy/energy dispersive spectroscopy (HR-TEM/EDS); and Mössbauer spectroscopy were employed as reported by previous studies in the literature [23,24]. The HR-TEM was performed based on the detailed methodology described by previous studies in the literature [25–27].

The use of HR-TEM provides a basis for critical examination of nanoparticles without affecting the samples. Furthermore, the low-cost geochemical investigations present various useful materials on the depositional conditions and coal pollution history [28,29], which could support knowledge on the origins and incidences of numerous PM. To acquire the main geological phases, the particles obtained were examined by X-ray powder diffraction (XRD) and Mössbauer spectroscopy. These techniques are capable of operating in a continuous conservative mode of acceleration by means of a relative counter filled with Xe-gas to 2 atm [30,31]. Hence, the UFP and NP samples of each separable size or class were also examined by FE-SEM and HR-TEM/EDS.

The morphology and geochemical conformations of the PM in the accumulated samples were examined by FE-SEM fitted with EDS under secondary electron (SE) and backscattered electron modes [32,33]. The SEM was operated at 15 kV accelerating voltage and 0.1 nA beam current. The EDS is a semi-quantitative apparatus typically employed to detect the chemical configurations of sampled compounds at 0.1 wt. % detection limit. The utilized EDS point-mode was carried out less than 15 kV voltage, 2 nA beam current, and 10-mm working distance. After stabilizing the energy spectrums, each elemental atomic and weight percentage was converted by X-ray counts. Similar SEM procedures have been described in the literature [24,30,31].

The elemental configurations of the NPs were investigated by HR-TEM combined with EDS and FFT [34,35]. The NPs were evaluated by 200 keV HR-TEM (Model: JEOL JEM-2010F, Japan) coupled with EDS (Model: Quantax 200, JEOL, Japan). The samples were separated and dissolved in several organic solvents through ultrasonic-sound suspension before being pipetted into Lacy Carbon films supported by Cu grids [36,37]. To prevent

contamination, the HR-TEM sample holder was prepared using an advanced plasma system (Model: Gatan Model 950). The HR-TEM point and lattice resolutions were; 0.194 nm and 0.1 nm, respectively [30,31].

Based on the geochemical confirmation, the potential NPs can be selected using the Inorganic Compound Powder Diffraction File (PDF) catalogue from the International Center for Diffraction Database. The PDFs of the selected nanominerals were applied to associate with the Fast Fourier Transform (FFT) patterns data to calibrate NPs. As observed by several authors in the literature [7,23,38,39], NPs are typically characterized by some crystal defects. The most notable include; additional disordering, shearing, or impurities that result in minor differences between the tested nanominerals and standard minerals in the PDF database [23,40].

The diffraction pattern indexes of the NPs, including interplanar spacing (d) and angle of crystal plane (<D_1, D_2>), were measured by Digital Micrograph software. Furthermore, the average data (from the PDF database) was correlated with the detected values to conclusively recognize the crystal(s) with the following restrictions: $|d_m - d_s| < 0.01$ nm (where d_s: standard d value, d_m: measured d value); $|<D_{m1}, D_{m2}> - <D_{s1}, D_{s2}>| < 3^\circ$ (where <D_{s1}, D_{s2}>: standard angle value; <D_{m1}, D_{m2}>: measured angle value). Furthermore, the indicators of the mineral face (hkl) of d_{s1}, d_{s2}, d_{s3} must coincide with the balance: $h_1k_1l_1 + h_2k_2l_2 = h_3k_3l_3$ (where $h_1k_1l_1$, $h_2k_2l_2$, and $h_3k_3l_3$ are the crystal faces of d_{s1}, d_{s2}, and d_{s3}, correspondingly). In addition, the <D_{s1}, D_{s2}> was computed by the cell considerations (a, b, c, α, β, γ) and the two recognized ($h_1k_1l_1$) and ($h_2k_2l_2$). The terms a, b, c are 3 clusters of edge lengths, whereas α, β, γ are the intersecting angles.

3. Results

3.1. Particulate Matter Analysis

The metal pin stub for sample collection did not detect any PHE contamination because it was covered with carbon tape. The results of this initial study provide a concise demonstration of how the metallic content of coal mine dust can change as the powder becomes thinner and more deeply inhaled. In addition, several PM containing PHEs were observed in the investigated zone (Table 1). As denoted above, the real atmosphere and the potential sources of various UFPs and NPs were examined directly to determine the observed compounds. The samples were analyzed without further sample treatment using non-destructive microscopic and SMPS methods. Moreover, the study of pollution history, depositional situation, and geochemical, may be vital to gain a detailed characterization of the NPs.

Table 1. Recognized compounds; and PHEs in the studied coal area.

Sample Names	PM 11	PM 12	PM 13	PM 14	PM 15	PM 16	PM 17	PM 18
Amorphous	B	B	B	B	B	B	B	B
Mineral								
Anatase	B	B		B	B	B	B	
Anhydrite	A, B			A, B		B		B
Alunogen	B			B		B		
Barite	B	B		B	B	B		
Calcite	B	A, B	A, B		A, B	A, B		A, B
Dolomite	B	A, B	A, B	B		A, B	B	B
Epsomite		B			B		B	B
Ferrohexahydrite	B	B, M	B, M	M		M	M	M
Gypsum	B, M	B	B	B	B		B	B

Table 1. *Cont.*

Sample Names	PM 11	PM 12	PM 13	PM 14	PM 15	PM 16	PM 17	PM 18
Hematite	B			B	B	B	B	B
Jarosite	B		B	B, M		B	B	B
Kaolinite	B, M	B	B, M		B, M	B, M	B, M	B, M
Melanterite	B, M	A, B	B	A, B	B	B	A	A
Mullite	A, B	B	M		M	M		
Pyrite	B, M	B				B	B	B
Quartz	B	B, M	M	M	B, M	A, B, M	A, B, M	A, B, M
Rutile	A, B, M		A, B	B	A, B	A, B	A, B	A, B
Siderite and Sphalerite	B		B		B	B	B	B
	B		B, M	M	M		B, M	B, M
Chemical Elements								
Al	E	E	E	E	E	E	E	E
As	E		E		E			E
Ba	E	E		E	E	E		E
Br	E		E		E		E	E
Ca	E	E	E	E	E	E	E	E
Cd	E	E	E	E	E	E	E	E
Cl	E			E	E		E	E
Cu	E	E	E			E	E	E
Co	E	E			E	E		
Cr		E	E	E		E	E	
Fe	E	E	E	E	E	E	E	E
Hg	E		E	E			E	E
Mn	E	E	E	E	E	E	E	E
Ni	E	E	E	E		E	E	E
Pb	E	E	E	E	E	E	E	
S	E			E			E	E
Sb	E		E	E		E	E	
Se	E		E	E		E	E	E
Ti	E	E	E	E	E	E	E	E
V	E		E			E	E	E
Zn			E					

* XRD = A; AM = B; M = Mössbauer spectroscopy; E = EDS.

Most of the PMs identified exist in the form of complex aggregates and separate UPFs. The NPs agglomerated to form new compounds, thus displaying a smooth and well-regulated morphology. As observed, the aggregates formed are asymmetrical and approximately equidimensional. Typically, the quality of most aggregates is dependent on the size and chemical heterogeneity of their UFPs components. The sizes range between hundreds and tens of nanometers based on rounded outlines [1,23,41]. In many cases, UFPs can maintain multifaceted geochemical histories during growth and development based on varying environmental circumstances. In this study, the UPFs determined by the analytical approach (Table 1) vary from very complexes aggregation of PHEs and

organic compounds (with numerous amorphous associations) to carbonaceous matter. According to Hochella et al. [42], related atmospheric NPs could grow into larger UFPs that act as cloud condensation nuclei and assist in light concentration, which dislocate global warming evolutions.

Furthermore, Table 1 presents the most abundant phases computed from the EDS mappings and quantitative analyses adopted in this study. The most prominent detected phases are linked with re-suspended powder or crustal/mine PM. Hence, the observed PMs (Figures 2–4) clearly illustrate the results of the detailed analytical approach used to compute the various phases stored on the applied SMPS. The EDS component mapping revealed that the combination of compounds frequently involves separate UPFs and NPs, which are alterable and rarely of similar geochemical structure. This analysis supports the point study for the enormous quantity of PMs.

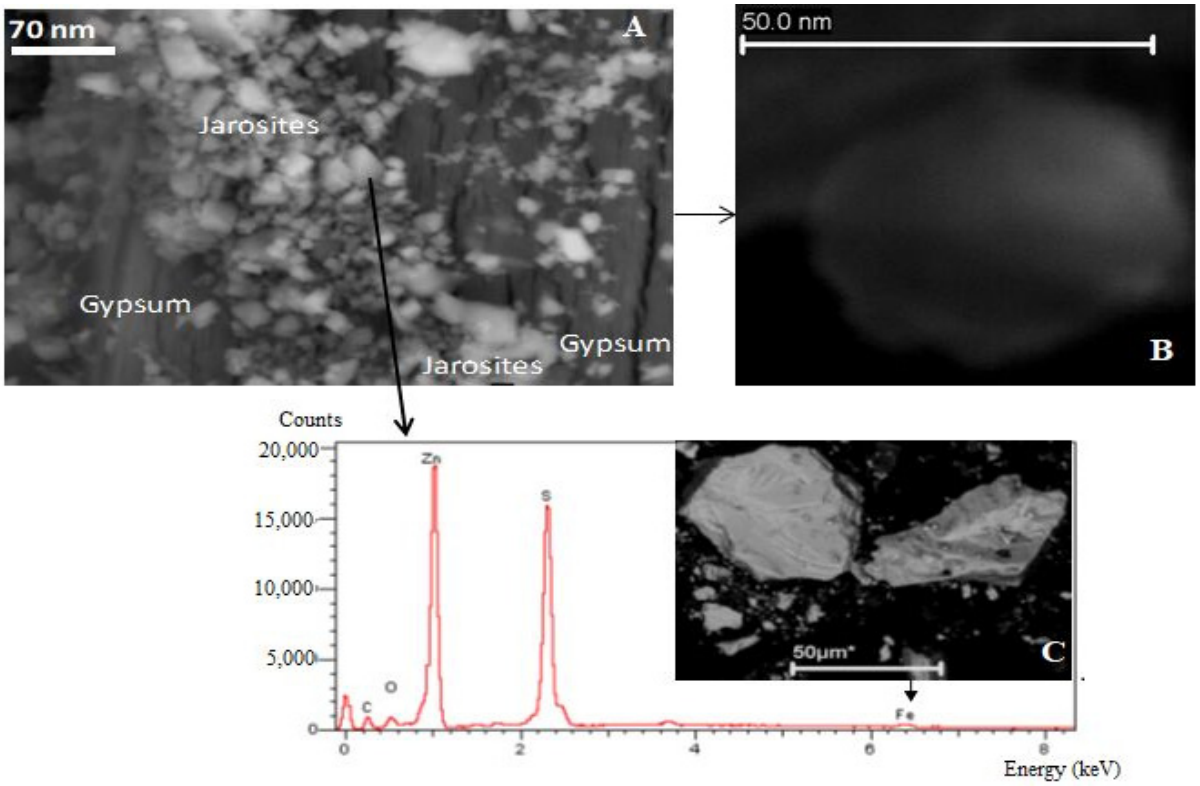

Figure 2. Compounds containing PHEs: (**A**) Jarosite; (**B**) Spherical amorphous particle around several jarosites and goethite minerals; (**C**) Sphalerite containing Fe in the crystalline structure in the PM 11–PM 18.

Furthermore, Table 1 shows the dates for the study of SMPS PM obtained from the restaurants in Brazilian coal mines. Based on the most abundant chemical components, it can be observed that all samples showed comparable sources. This is evident in the broad geochemical relationships with aluminum, calcium, carbon, iron, magnesium, manganese, and silicon. In the coarser accumulated PM, calcium has the highest composition. However, the Ca cation in the NPs portions is reduced in proportion and surpassed in mass by Al and Fe, which regularly increases in total accumulated particles from PM_{10} to PM_1. Majority of the abundant chemical components display an analogous behavior to aluminum, iron, magnesium, and particularly potassium and sodium all attaining highest levels in the PM_1. The EDS, coupled to TEM and SEM investigation of the PM indicates that the principal cause of sulphur in the total accumulated particles is in the form of organic matter NPs and sulphides UFPs. However, the XRD analysis revealed that the accumulated particles corroborate the existence of quartz, clays, pyrite, and Ca-minerals (Table 1).

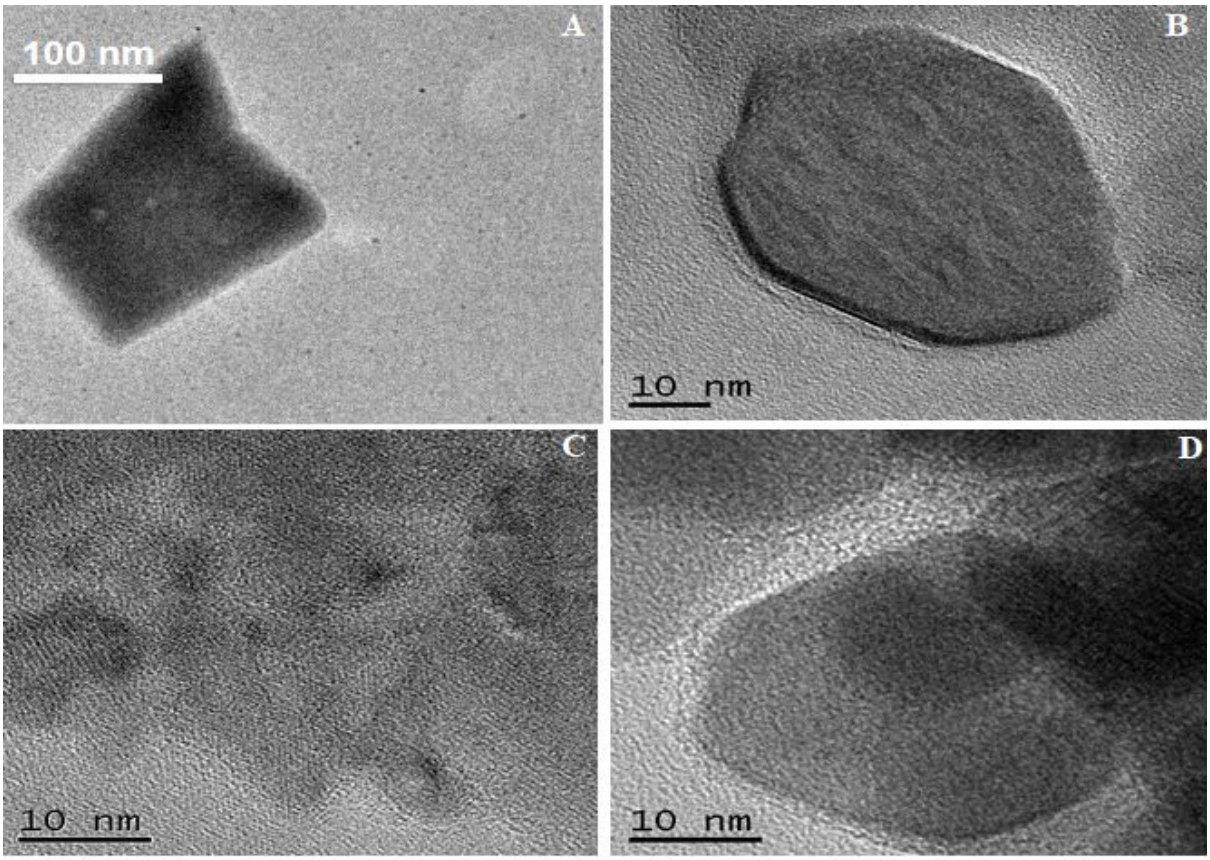

Figure 3. Selected identified NPs: (**A**) Angular carbonaceous matter including As and Se; (**B**) Spherical nano-kaolinite; (**C**) Fe-amorphous and crystalline mixed with carbonaceous matter containing Pb; (**D**) Hematite containing Pb.

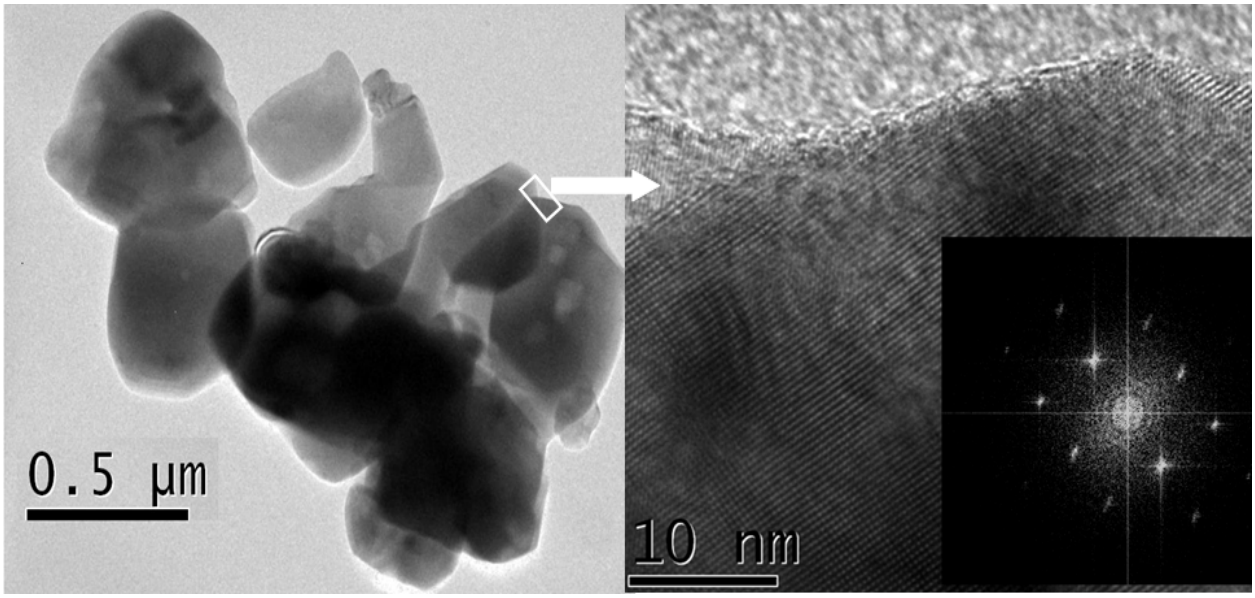

Figure 4. Massive rutile agglomerate and crystalline detail HR-TEM image contain FFT (for identification).

3.2. Electron Beam Analysis

As illustrated in Table 1, several samples contained pyrite, jarosite, and amorphous phases. The FE-SEM, FIB-SEM and HR-TEM results showed an association streak between the particles illustrated in Figure 2, particularly between spherical PM and pyrite-containing

sulphates. Similar results were previously reported by coal cleaning rejects (CCRs) studies [43,44]. This indicates that such CCRs are easily inhaled by coal miners and the local population residing near the mines.

Another important correlation is between the sphalerite containing Fe in this crystalline mineral structure and the siderite crystals. This observation shows that the geological processes in the study area enhance the formation of minerals during coalification. Hence, the dust extracted from the coal can be inhaled, as illustrated in the Figures 2–5 of the particles examined in this study. The Fe-NPs identified by HR-TEM and FIB-SEM/EDS can be chemically transformed into other iron-sulphates/hydroxides such as displays of goethite [34,37], which occur either in the vicinity or by interaction with Fe-sulphate. Hematite (Figure 3D) appears in parallel PM, which has been partly transformed into Fe-amorphous NPs (Figure 3C). These multifaceted NP groups of Fe-particles contain Pb as identified by HR-TEM and Mössbauer Spectroscopy. Furthermore, the Fe-containing-Pb particles occur as amorphous to mineral PMs formed from Al-Si-O-K-Mg and/or carbonaceous matter.

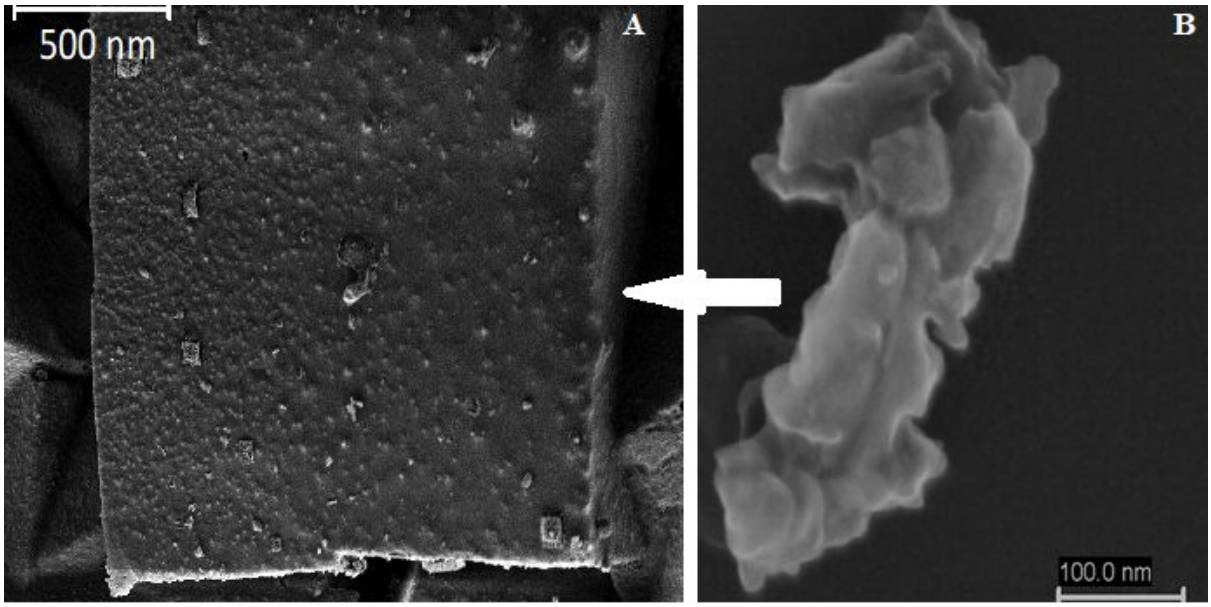

Figure 5. (**A**) Sallammoniac and (**B**) siderite as depicted in HR-TEM image contain FFT (for identification).

The proposed low-cost analytical sampling and subsequent analyses also identified many other PM containing PHEs, as illustrated in Figures 3–5. The HR-TEM, coupled with EDS, SAED and FFT investigation of Ti-compounds, confirm the existence of anatase and rutile (Figure 4). These Ti-phases are significantly toxic according to several toxicological studies, either in concentrated or dispersed in coal and coal by-products [24,45,46].

The proportions of Ca and carbon in the various PM sections were evaluated using the SMPS. For the studied coal mine, the findings indicate that the airborne calcareous or carbonaceous constituents of the coal mine dust are not the most concentrated or inhalable UFPs. In its place, the cumulative proportions of the Al-Fe-K-Mg-Mn-Na-P indicate the occurrence of UFPs clays and oxides in the PM_1 compared to the Ca-Fe-carbonates. This interpretation indicates a hypothesis has been confirmed by the FIB-SEM/EDS, FE-SEM/EDS and HR-TEM/SAED/FFT/EDS analyses. Hence, the confirmation presents a functional characterization of the PM developed from the UFPs and NPs in coal mines.

Some previous authors have clarified the associations between PM sources and population health, including respiratory and mortality [47]. However, no scientific research has estimated these associations during the winter period in Brazil, specifically in coal mining areas.

In this work, several minerals such as iron sulfides and some organic phases were identified as having significant associations with respiratory diseases. Particles such as sallammoniac (Figure 5A) and siderite containing amorphous superficial particles (Figure 5B) are clearly derived from spontaneous coal combustion or a variety of high temperature thermal history [25]. Hence, the coal dust or soil processing actions are consequently re-suspended or emitted directly into the food/restaurant areas of the coal mining areas in Brazil.

4. Discussion

The sources of the tested dust (transportation, mining, and conveyor), whether it is only coal, or surrounding rocks, soil etc were abundant in the areas under study. As we can see in the different figures, minerals and multiple complex amorphous phases of different compositions were detected. Although the greatest impact is in the mining and coal power plant area, transport also implies serious environmental impacts throughout its journey. The exposure of coal to atmospheric conditions promotes sulphide oxidation that releases enormous sulphate loads as well as Ca^{2+}, K^{+}, Mg^{2+}, Cl^{-} and Al^{3+} [30].

The ultrafine and nano compounds (both minerals and amorphous phases) identified in this study capture potential hazardous elements (PHEs) in the nanometer size range (Figures 2–5). HR-TEM is a powerful analytical technique that provides a better understanding of the detailed chemistry of the potentially strongly bioreactive component of atmospheric particulate matter [38,48]. The combined X-Ray Diffraction (XRD) and advanced electron microscopy (AM) techniques, demonstrates the importance of nanomineralogy in understanding different circumstances of coal contamination [49].

The diameter (≈0.5–100 nm) of the nano-spheres posed severe concerns linked with environmental impact and human health through breathing. The harmful developments in the lung and heart that follow particulate air pollution inhalation are related to the chemical composition of the particles [50].

The spheres below 1 nm are extremely troublesome for human health, because it can penetrate the lungs and bloodstream [51–53]. Titanium dioxide is reported to be an aggravating factor for environment and human health [54]. Anatase and rutile nanoparticles are purportedly activate adverse pulmonary responses in susceptible animals [52]. The anatase TiO_2 nanoparticles produce more free radicals than rutile form and, consequently, higher toxicity than the rutile TiO_2 nanoparticle. The anatase titanium nanoparticles (Ti-NPs) are one of the foremost sources of inflammation and cytotoxicity [55]. The distribution of PHEs among the Ti-NPs aggregates was controlled by carbonaceous matter and amorphous silica [56].

Correspondingly, iron oxide (hematite) and iron carbonate (sallamoniac and siderite) nanoparticles detected in this study (Figure 5), contain hazardous elements (such as As, Se and Pb) that could have momentous health effects. Relatedly in-vivo studies have showed that pulmonary contact with iron oxide nanoparticles can cause genotoxicity and inflammation along with effects such as pulmonary and extra-pulmonary fibrosis [57]. These have also been indicated in the production of damaging reactive oxygen species (ROS) [58]. Furthermore, hematite nanoparticles improved the growth of soil bacteria [59]. Characteristic jarosite, gypsum, geothite minerals and sphelarite were identified containing potential hazardous elements (Figure 2). The cubic-shaped jarosite appears to be a pseudomorph after pyrite. Removal of water from jarosite can result to the formation of less-hydrous Fe sulfates and hematite [60]. Silva et al. [61] reported the immobilisation of Fe and Pb due to precipitation as jarosite or hematite in the case of Fe or as a sulphate in case of Pb. The COVID-19 mortality is found to be partially driven by the long term exposure to particulate matter ($PM_{2.5}$) and delayed for 18 days after high exposure to particulate matter ($PM_{2.5}$) [62].

5. Conclusions

The study presented a low-cost method that effectively documents the presence of several minerals and amorphous phases in the air and posed health risks to mine workers. Furthermore, the purpose of the study was to identify the NPs and UFPS groups, which are critical air contaminants related to several categories of respiratory disorders. The advanced surface techniques used in the study are required to examine the chemical composition at the nanoscale in order to create awareness for the inherent health hazards due to potential exposure. The chemical composition of nanoparticle/nano minerals strive for improve knowledge on its adverse effects on human health and the environment [55]. The mine workers are exposed to wind-blown particulate matter that contains nanoparticles as well as potentially hazardous elements (PHEs).

The study further demonstrated the prospects of identifying a broad spectrum of PHEs, which could become heavily concentrated in the finest and inhalable fraction of coal mine dust in the air. Such elements (e.g., Table 1) are recognized by the ability to induce adverse effects on human health and are therefore of concern at high concentrations.

The findings also showed that Brazilian coal is geochemically complex and highly variable [46,63–65]. Therefore, future studies will be considered to examine the possible health toxicities and optimize the fine and inhalable fraction of coal mine dust. Lastly, the comparative analysis presented in this scientific research show that coal mine dust is chemically different from the thicker air materials present in the mine air.

Author Contributions: M.L.S.O.; S.A.A.: Writing—original draft. Data Curation. B.B.N.; G.L.D.: Writing—review & editing. All authors have read and agreed to the published version of the manuscript.

Funding: This research did not received external funding.

Institutional Review Board Statement: The study was conducted in accordance with the Declaration of Helsinki, and approved by the Institutional Review.

Informed Consent Statement: Informed consent was obtained from all subjects involved in the study.

Data Availability Statement: Not applicable.

Acknowledgments: The authors would like to acknowledge support from material support and technical assistance of the Brazilian National Council for Scientific and Technological Development (CNPQ) and Coordenação de Aperfeiçoamento de Pessoal de Nível Superior (CAPES) of Brazil.

Conflicts of Interest: The authors declare that they have no known competing financial interests or personal relationships that could have appeared to influence the work reported in this paper.

References

1. Munawer, M.E. Human health and environmental impacts of coal combustion and post-combustion wastes. *J. Sustain. Min.* **2018**, *17*, 87–96. [CrossRef]
2. Gent, J.F.; Triche, E.W.; Holford, T.R.; Belanger, K.; Bracken, M.B.; Beckett, W.S.; Leaderer, B.P. Association of low-level ozone and fine particles with respiratory symptoms in children with asthma. *JAMA* **2003**, *290*, 1859–1867. [PubMed]
3. Manisalidis, I.; Stavropoulou, E.; Stavropoulos, A.; Bezirtzoglou, E. Environmental and health impacts of air pollution: A review. *Front. Public Health* **2020**, *8*, 14. [CrossRef]
4. Ramírez, O.; de la Campa, A.M.S.; Amato, F.; Moreno, T.; Silva, L.; de la Rosa, J.D. Physicochemical characterization and sources of the thoracic fraction of road dust in a Latin American megacity. *Sci. Total Environ.* **2019**, *652*, 434–446. [CrossRef] [PubMed]
5. Blackley, D.J.; Halldin, C.N.; Laney, A.S. Continued increase in prevalence of coal workers' pneumoconiosis in the United States, 1970–2017. *Am. J. Public Health* **2018**, *108*, 1220–1222. [CrossRef]
6. Moreno, T.; Trechera, P.; Querol, X.; Lah, R.; Johnson, D.; Wrana, A.; Williamson, B. Trace element fractionation between PM_{10} and $PM_{2.5}$ in coal mine dust: Implications for occupational respiratory health. *Int. J. Coal Geol.* **2019**, *203*, 52–59. [CrossRef]
7. Garcia, K.O.; Teixeira, E.C.; Agudelo-Castañeda, D.M.; Braga, M.; Alabarse, P.G.; Wiegand, F.; Kautzmann, R.M.; Silva, L.F. Assessment of nitro-polycyclic aromatic hydrocarbons in PM_1 near an area of heavy-duty traffic. *Sci. Total Environ.* **2014**, *479*, 57–65. [CrossRef]
8. Schneider, I.L.; Teixeira, E.C.; Agudelo-Castañeda, D.M.; e Silva, G.S.; Balzaretti, N.; Braga, M.F.; Oliveira, L.F.S. FTIR analysis and evaluation of carcinogenic and mutagenic risks of nitro-polycyclic aromatic hydrocarbons in PM 1.0. *Sci. Total Environ.* **2016**, *541*, 1151–1160. [CrossRef]

9. Poenar, D.P. Microfluidic and micromachined/MEMS devices for separation, discrimination and detection of airborne par-ticles for pollution monitoring. *Micromachines* **2019**, *10*, 483.
10. Azam, S.; Mishra, D.P. Effects of particle size, dust concentration and dust-dispersionair pressure on rock dust inertant requirement for coal dust explosion suppression in underground coal mines. *Process Saf. Environ. Prot.* **2019**, *126*, 35–43.
11. Haas, E.J. Using self-determination theory to identify organizational interventions to support coal mineworkers' dust-reducing practices. *Int. J. Min. Sci. Technol.* **2019**, *29*, 371–378. [CrossRef]
12. Su, X.; Ding, R.; Zhuang, X. Characteristics of dust in coal mines in central north China and its research significance. *ACS Omega* **2020**, *5*, 9233–9250. [PubMed]
13. Farmer, J.G.; Broadway, A.; Cave, M.; Wragg, J.; Fordyce, F.; Graham, M.C.; Ngwenya, B.T.; Bewley, R.J. A lead isotopic study of the human bioaccessibility of lead in urban soils from Glasgow, Scotland. *Sci. Total Environ.* **2011**, *409*, 4958–4965. [CrossRef] [PubMed]
14. Amirah, M.; Afiza, A.; Faizal, W.; Nurliyana, M.; Laili, S. Human health risk assessment of metal contamination through consumption of fish. *J. Environ. Pollut. Hum. Health* **2013**, *1*, 1–5.
15. Akinyemi, S.A.; Gitari, W.M.; Petrik, L.F.; Nyakuma, B.B.; Hower, J.C.; Ward, C.R.; Oliveira, M.L.; Silva, L.F. Environmental evaluation and nano-mineralogical study of fresh and unsaturated weathered coal fly ashes. *Sci. Total Environ.* **2019**, *663*, 177–188.
16. Ezemonye, L.I.; Adebayo, P.O.; Enuneku, A.A.; Tongo, I.; Ogbomida, E. Potential health risk consequences of heavy metal concentrations in surface water, shrimp (*Macrobrachium macrobrachion*) and fish (*Brycinus longipinnis*) from Benin River, Nigeria. *Toxicol. Rep.* **2019**, *6*, 1–9. [CrossRef]
17. Pan, L.; Golden, S.; Assemi, S.; Sime, M.; Wang, X.; Gao, Y.; Miller, J. Characterization of particle size and composition of respirable coal mine dust. *Minerals* **2021**, *11*, 276. [CrossRef]
18. Abbasi, B.; Wang, X.; Chow, J.; Watson, J.; Peik, B.; Nasiri, V.; Riemenschnitter, K.; Elahifard, M. Review of respirable coal mine dust characterization for mass concentration, size distribution and chemical composition. *Minerals* **2021**, *11*, 426. [CrossRef]
19. Mu, M.; Li, B.; Zou, Y.; Wang, W.; Cao, H.; Zhang, Y.; Sun, Q.; Chen, H.; Ge, D.; Tao, H.; et al. Coal dust exposure triggers heterogeneity of transcriptional profiles in mouse pneumoconiosis and vitamin D remedies. *Part. Fibre Toxicol.* **2022**, *19*, 1–21. [CrossRef]
20. Liu, T.; Liu, S. The impacts of coal dust on miners' health: A review. *Environ. Res.* **2020**, *190*, 109849. [CrossRef]
21. Silva, L.F.; Milanes, C.; Pinto, D.; Ramirez, O.; Lima, B.D. Multiple hazardous elements in nanoparticulate matter from a Caribbean industrialized atmosphere. *Chemosphere* **2020**, *239*, 124776. [CrossRef] [PubMed]
22. Lindsley, W.G.; Green, B.J.; Blachere, F.M.; Martin, S.B.; Law, B.; Jensen, P.; Schafer, M. *Sampling and Characterization of Bioaerosols. NIOSH Manual of Analytical Methods*, 5th ed.; National Institute for Occupational Safety and Health: Cincinnati, OH, USA, 2017.
23. Cerqueira, B.; Vega, F.A.; Silva, L.; Andrade, M.L. Effects of vegetation on chemical and mineralogical characteristics of soils developed on a decantation bank from a copper mine. *Sci. Total Environ.* **2012**, *421*, 220–229. [CrossRef] [PubMed]
24. Nordin, A.P.; da Silva, J.; de Souza, C.T.; Niekraszewicz, L.A.; Dias, J.; da Boit, K.; Oliveira, M.L.; Grivicich, I.; Garcia, A.L.H.; Oliveira, L.F.S.; et al. In vitro genotoxic effect of secondary minerals crystallized in rocks from coal mine drainage. *J. Hazard. Mater.* **2018**, *346*, 263–272. [CrossRef] [PubMed]
25. Ribeiro, J.; Flores, D.; Ward, C.; Silva, L.F. Identification of nanominerals and nanoparticles in burning coal waste piles from Portugal. *Sci. Total Environ.* **2010**, *408*, 6032–6041. [CrossRef]
26. Sehn, J.L.; de Leão, F.B.; da Boit, K.; Oliveira, M.; Hidalgo, G.E.; Sampaio, C.H.; Silva, L. Nanomineralogy in the real world: A perspective on nanoparticles in the environmental impacts of coal fire. *Chemosphere* **2016**, *147*, 439–443. [CrossRef]
27. Rojas, J.C.; Sánchez, N.E.; Schneider, I.; Oliveira, M.L.; Teixeira, E.C.; Silva, L.F. Exposure to nanometric pollutants in primary schools: Environmental implications. *Urban Clim.* **2019**, *27*, 412–419. [CrossRef]
28. Gitari, M.W.; Akinyemi, S.A.; Ramugondo, L.; Matidza, M.; Mhlongo, S.E. Geochemical fractionation of metals and metalloids in tailings and appraisal of environmental pollution in the abandoned Musina Copper Mine, South Africa. *Environ. Geochem. Health* **2018**, *40*, 2421–2439. [CrossRef]
29. Akinyemi, S.A.; Gitari, W.M.; Thobakgale, R.; Petrik, L.F.; Nyakuma, B.B.; Hower, J.C.; Ward, C.R.; Oliveira, M.L.S.; Silva, L.F.O. Geochemical fractionation of hazardous elements in fresh and drilled weathered South African coal fly ashes. *Environ. Geochem. Health* **2020**, *42*, 2771–2788. [CrossRef]
30. Silva, L.; Izquierdo, M.; Querol, X.; Finkelman, R.B.; Oliveira, M.; Wollenschlager, M.; Towler, M.; Pérez-López, R.; Macias, F. Leaching of potential hazardous elements of coal cleaning rejects. *Environ. Monit. Assess.* **2010**, *175*, 109–126. [CrossRef]
31. Silva, L.; Macias, F.; Oliveira, M.; da Boit, M.K.; Waanders, F.B. Coal cleaning residues and Fe-minerals implications. *Environ. Monit. Assess.* **2010**, *172*, 367–378. [CrossRef]
32. Oliveira, M.L.; da Boit, K.; Pacheco, F.; Teixeira, E.C.; Schneider, I.L.; Crissien, T.J.; Pinto, D.C.; Oyaga, R.M.; Silva, L.F. Multifaceted processes controlling the distribution of hazardous compounds in the spontaneous combustion of coal and the effect of these compounds on human health. *Environ. Res.* **2018**, *160*, 562–567. [PubMed]
33. Oliveira, M.L.; da Boit, K.; Schneider, I.L.; Teixeira, E.C.; Borrero, T.J.C.; Silva, L.F. Study of coal cleaning rejects by FIB and sample preparation for HR-TEM: Mineral surface chemistry and nanoparticle-aggregation control for health studies. *J. Clean. Prod.* **2018**, *188*, 662–669. [CrossRef]
34. Meyer, H.; Meischein, M.; Ludwig, A. Rapid assessment of sputtered nanoparticle ionic liquid combinations. *ACS Comb. Sci.* **2018**, *20*, 243–250. [CrossRef] [PubMed]

35. Garzón-Manjón, A.; Meyer, H.; Grochla, D.; Löffler, T.; Schuhmann, W.; Ludwig, A.; Scheu, C. Controlling the amorphous and crystalline state of multinary alloy nanoparticles in an ionic liquid. *Nanomaterials* **2018**, *8*, 903. [CrossRef]
36. Ribeiro, J.; Valentim, B.; Ward, C.; Flores, D. Comprehensive characterization of anthracite fly ash from a thermo-electric power plant and its potential environmental impact. *Int. J. Coal Geol.* **2011**, *86*, 204–212. [CrossRef]
37. Quispe, D.; Pérez-López, R.; Silva, L.F.; Nieto, J.M. Changes in mobility of hazardous elements during coal combustion in Santa Catarina power plant (Brazil). *Fuel* **2012**, *94*, 495–503. [CrossRef]
38. Silva, L.F.; Hower, J.C.; Izquierdo, M.; Querol, X. Complex nanominerals and ultrafine particles assemblages in phosphogypsum of the fertilizer industry and implications on human exposure. *Sci. Total Environ.* **2010**, *408*, 5117–5122.
39. Akinyemi, S.; Akinlua, A.; Gitari, W.; Khuse, N.; Eze, P.; Akinyeye, R.; Petrik, L. Natural weathering in dry disposed ash dump: Insight from chemical, mineralogical and geochemical analysis of fresh and unsaturated drilled cores. *J. Environ. Manag.* **2012**, *102*, 96–107. [CrossRef]
40. Arenas-Lago, D.; Vega, F.; Silva, L.; Andrade, M. Soil interaction and fractionation of added cadmium in some Galician soils. *Microchem. J.* **2013**, *110*, 681–690. [CrossRef]
41. Giemsa, E.; Soentgen, J.; Kusch, T.; Beck, C.; Münkel, C.; Cyrys, J.; Pitz, M. Influence of local sources and meteorological parameters on the spatial and temporal distribution of ultrafine particles in Augsburg, Germany. *Front. Environ. Sci.* **2021**. [CrossRef]
42. Hochella, M.F.; Mogk, D.W.; Ranville, J.; Allen, I.C.; Luther, G.W.; Marr, L.C.; McGrail, B.P.; Murayama, M.; Qafoku, N.P.; Rosso, K.M.; et al. Natural, incidental, and engineered nanomaterials and their impacts on the Earth system. *Science* **2019**, *363*, eaau8299. [CrossRef] [PubMed]
43. Oliveira, M.L.; Ward, C.; Izquierdo, M.; Sampaio, C.H.; de Brum, I.A.; Kautzmann, R.M.; Sabedot, S.; Querol, X.; Silva, L.F. Chemical composition and minerals in pyrite ash of an abandoned sulphuric acid production plant. *Sci. Total Environ.* **2012**, *430*, 34–47. [CrossRef] [PubMed]
44. Shahhoseiny, M.; Ardejani, F.D.; Shafaei, S.Z.; Singh, R.; Shokri, B.J. Geochemical characterisation of a pyrite containing coal washing refuse pile produced by the Anjir Tangeh coal washing plant in Zirab, Mazandaran province, Northern Iran. In Proceedings of the 11th International Mine Water Association Congress—Mine Water—Managing the Challenges (IMWA 2011), Aachen, Germany, 4–11 September 2011.
45. Gasparotto, J.; Chaves, P.R.; Martinello, K.D.B.; da Rosa-Siva, H.T.; Bortolin, R.C.; Silva, L.; Rabelo, T.K.; da Silva, J.; da Silva, F.R.; Nordin, A.P.; et al. Obese rats are more vulnerable to inflammation, genotoxicity and oxidative stress induced by coal dust inhalation than non-obese rats. *Ecotoxicol. Environ. Saf.* **2018**, *165*, 44–51. [CrossRef]
46. Gasparotto, J.; Chaves, P.R.; Martinello, K.D.B.; Oliveira, L.F.S.; Gelain, D.P.; Moreira, J.C.F. Obesity associated with coal ash inhalation triggers systemic inflammation and oxidative damage in the hippocampus of rats. *Food Chem. Toxicol.* **2019**, *133*, 110766. [CrossRef]
47. Ostro, B.; Tobias, A.; Querol, X.; Alastuey, A.; Amato, F.; Pey, J.; Pérez, N.; Sunyer, J. The effects of particulate matter sources on daily mortality: A case-crossover study of Barcelona, Spain. *Environ. Health Perspect.* **2011**, *119*, 1781–1787. [CrossRef]
48. Silva, L.; Moreno, T.; Querol, X. An introductory TEM study of Fe-nanominerals within coal fly ash. *Sci. Total Environ.* **2009**, *407*, 4972–4974. [CrossRef]
49. Silva, L.F.O.; Pinto, D.; Dotto, G.L.; Hower, J.C. Nanomineralogy of evaporative precipitation of efflorescent compounds from coal mine drainage. *Geosci. Front.* **2021**, *12*, 101003.
50. Gurgueira, S.; Lawrence, J.; Brent, C.; Krishna, M.; Gonzalez-Flecha, B. Rapid increases in the steady-state concentration of reactive oxygen species in the lungs and heart after particulate air pollution inhalation. *Environ. Health Perspect.* **2002**, *110*, 749–755.
51. Ribeiro, J.; Taffarel, S.R.; Sampaio, C.H.; Flores, D.; Silva, L.F. Mineral speciation and fate of some hazardous contaminants in coal waste pile from anthracite mining in Portugal. *Int. J. Coal Geol.* **2013**, *109*, 15–23.
52. Silva, L.F.; DaBoit, K.; Sampaio, C.H.; Jasper, A.; Andrade, M.L.; Kostova, I.J.; Waanders, F.B.; Henke, K.R.; Hower, J.C. The occurrence of hazardous volatile elements and nanoparticles in Bulgarian coal fly ashes and the effect on human health exposure. *Sci. Total Environ.* **2012**, *416*, 513–526. [CrossRef]
53. Silva, L.F.O.; Jasper, A.; Andrade, M.L.; Sampaio, C.H.; Dai, S.; Li, X.; Li, T.; Chen, W.; Wang, X.; Liu, H.; et al. Applied investigation on the interaction of hazardous elements binding on ultrafine and nanoparticles in Chinese anthracite-derived fly ash. *Sci. Total Environ.* **2012**, *419*, 250–264. [PubMed]
54. Silva, L.F.O.; Hower, J.C.; Dotto, G.L.; Marcos, L.S.; Oliveira, M.L.S.; Moreno, A.L. Nanoparticles from evaporite materials in Colombian coal mine drainages. *Int. J. Coal Geol.* **2020**, *230*, 103588.
55. Iavicoli, I.; Leso, V.; Bergamaschi, A. Toxicological effects of titanium dioxide nanoparticles: A review of in vivo studies. *J. Nanomater.* **2012**, *2012*, 1–36. [CrossRef]
56. Silva, L.F.O.; Hower, J.C.; Dotto, G.L.; Oliveira, M.L.S.; Pinto, D. Titanium nanoparticles in sedimented dust aggregates from urban children's parks around coal ashes wastes. *Fuel* **2021**, *285*, 119162.
57. Yang, Y.; Chen, B.; Hower, J.; Schindler, M.; Winkler, C.; Brandt, J.; di Giulio, R.; Ge, J.; Liu, M.; Fu, Y.; et al. Discovery and ramifications of incidental Magnéli phase generation and release from industrial coal-burning. *Nat. Commun.* **2017**, *8*, 1–11. [CrossRef]

58. Kornberg, T.; Stueckle, T.; Antonini, J.; Rojanasakul, Y.; Castranova, V.; Yang, Y.; Wang, L. Potential toxicity and under-lying mechanisms associated with pulmonary exposure to iron oxide nanoparticles: Conflicting literature and unclear risk. *Nanomaterials* **2017**, *7*, 307.
59. Maher, B.A.; Ahmed, I.A.; Karloukovski, V.; MacLaren, D.A.; Foulds, P.G.; Allsop, D.; Mann, D.M.; Torres-Jardón, R.; Calderon-Garciduenas, L. Magnetite pollution nanoparticles in the human brain. *Proc. Natl. Acad. Sci. USA* **2016**, *113*, 10797–10801.
60. Rajendran, K.; Sen, S.; Suja, G.; Senthil, S.L.; Kumar, T.V. Evaluation of cytotoxicity of hematite nanoparticles in bacteria and human cell lines. *Colloids Surf. B Biointerfaces* **2017**, *157*, 101–109. [CrossRef]
61. Silva, L.F.O.; Querol, X.; da Boit, K.M.; Fdez-Ortiz de Vallejuelo, S.; Madariaga, J.M. Brazilian coal mining residues and sulphide oxidation by Fenton's reaction: An accelerated weathering procedure to evaluate possible environmental im-pact. *J. Hazard. Mater.* **2011**, *186*, 516–525.
62. Shao, L.; Cao, Y.; Jones, T.; Santosh, M.; Silva, L.F.; Ge, S.; da Boit, K.; Feng, X.; Zhang, M.; Bérubé, K. COVID-19 mortality and exposure to airborne $PM_{2.5}$: A lag time correlation. *Sci. Total Environ.* **2021**, *806*, 151286. [CrossRef]
63. Silva, L.F.O.; Oliveira, M.L.S. *Nanominerals and Ultrafine Particles from Brazilian Coal Fires*; Elsevier: Amsterdam, The Netherlands, 2015; Volume 3.
64. Cutruneo, C.M.N.L.; Oliveira, M.L.S.; Ward, C.R.; Hower, J.C.; de Brum, I.A.S.; Sampaio, C.H.; Kautzmann, R.M.; Taffarel, S.R.; Teixeira, E.C.; Silva, L.F.O. A mineralogical and geochemical study of three Brazilian coal cleaning rejects: Demonstration of electron beam applications. *Int. J. Coal Geol.* **2014**, *130*, 33.
65. Dias, C.L.; Oliveira, M.L.S.; Hower, J.C.; Taffarel, S.R.; Kautzmann, R.M.; Silva, L.F.O. Nanominerals and ultrafine particles from coal fires from Santa Catarina, South Brazil. *Int. J. Coal Geol.* **2014**, *122*, 50–60.